Holocene palaeoceanographic evolution off West Greenland

K. Perner[1*], M. Moros[1], A. Jennings[2], J.M. Lloyd[3], K.L. Knudsen[4]

1 Leibniz Institute for Baltic Sea Research Warnemuende, Department of Marine Geology, Germany

2 Instaar and Department of Geological Sciences, University of Colorado, Boulder, USA

3 Durham University, Department of Geography, UK

4 Department of Geoscience, Aarhus University, DK-8000 Aarhus, DK

*corresponding author: kerstin.perner@io-warnemuende.de

Keywords: benthic foraminifera, WGC, IC, EGC, ocean forcing, Holocene

(A) Abstract

Benthic foraminiferal assemblages from a core southwest of Disko Bugt provide a Holocene perspective (last ~7 ka BP) on ice-sheet/ocean interactions between the West Greenland Current (WGC) and the West Greenland ice sheet. Changes in the fauna reveal significant variations in the water mass properties (temperature and salinity) of the WGC through time.

From 7.3 to 6.3 ka BP, a relatively warm/strong WGC influences ice sheet melt in Disko Bugt and causes enhanced meltwater production, resulting in low surface water productivity. The most favourable oceanographic conditions occur from 5.5 to 3.5 ka BP, associated with 'thermal optimum-like' conditions, encompassing minimum ice sheet extent in the Disko Bugt area. These conditions are attributed to: i) reduced meltwater influence as the ice sheet is land based and ii) enhanced contribution of warm/saline water masses from the Irminger Current to the WGC. The transition into the late Holocene (last ~3.5 ka BP) is characterized by a cooling of oceanographic conditions, caused by increased advection of cold/low-salinity water masses from the East Greenland Current. A longer-term late Holocene cooling trend within the WGC is attributed to the onset of Neoglacial cooling within the North Atlantic region. Superimposed on this cooling trend, multi-centennial scale variability within the WGC matches reconstructions from a nearby coring site in Disko Bugt as follows: i) cooling at ~2.5 ka BP, linked to the 2.7 ka BP 'cooling event'; ii) a warm phase centred at 1.8 ka BP, associated with the Roman Warm Period; iii) slight warming between 1.4 and 0.9 ka BP, linked to the Medieval Climate Anomaly; iv) severe cooling of the WGC after 0.9 ka BP, culminating at 0.3 ka BP during the Little Ice Age.

We show that multi-centennial scale paleoceanographic variability along the West Greenland margin is driven by ocean forcing, i.e. variations in the relative

contribution of Atlantic (Irminger Current) and Polar (East Greenland Current) water masses to the WGC during the last ~7 ka BP, influencing ice sheet dynamics.

(A) Introduction

Over the past two decades a negative mass balance and increased surface melting of the Greenland Ice Sheet (GIS), accompanied by enhanced acceleration of many of Greenland's marine terminating outlet glaciers (e.g. Jakobshavn Isbræ, Helheim, Kangerdlugssuaq) has been identified (Zwally et al., 2002; Rignot and Kanagaratnam, 2006; Moon and Joughin, 2008; Joughin et al., 2008; Howat et al., 2007, 2008; 2011; Straneo et al., 2010). Recent studies have suggested that ocean forcing may exert an important control on modern ice sheet dynamics by the influence of warmer ocean conditions (e.g. Thomas, 2004; Joughin et al., 2004; Bindschadler, 2006; Holland et al., 2008).

The Disko Bugt region in West Greenland is a key area to investigate the influence of ocean forcing on GIS behaviour. This region has a relatively wide shelf area and contains high-resolution sedimentary archives with the potential for records to obtain the interaction between oceanographic variability and ice sheet behaviour. The modern hydrographic conditions of the region are dominated by the West Greenland Current (WGC, Figure 1). The water mass composition of the WGC is linked to the large-scale North Atlantic climate system. Recent studies show that on a multi-decadal timescale, temperature changes within the WGC have a profound impact on subsurface melting of Disko Bugt outlet glaciers (e.g. Jakobshavn Isbræ), at least during the last 60 years (Holland et al., 2008; Rignot et al., 2010; Lloyd et al., 2011). Ice sheet limits in central West Greenland are uncertain during the Last Glacial Maximum (LGM), but it has been suggested that ice streams may have extended to the shelf edge along deep cross shelf troughs in the Disko Bugt region (see Funder et al., 2011 and references there in). Limited evidence reported re-appearance of the WGC in Disko Bugt from *c.* 9 to 10 ka BP (Funder and Weidick, 1991; Lloyd et al., 2005). Marine (Lloyd et al., 2005; Hogan et al., 2011) and terrestrial (Weidick and Bennicke, 2007; Briner et al., 2010; Young et al., 2011) studies suggest that Jakobshavn Isbræ had retreated into the Isfjord by *c.* 7.8 ka BP. There are, however, no high resolution records available spanning the period of ice retreat (after 8 ka BP) and minimum ice sheet extend (6 to 4 ka BP; e.g. Weidick and Bennike, 2007; Briner et al., 2010) documenting the paleoceanographic evolution of Disko Bugt (West Greenland).

To assess and understand the link between oceanic forcing and ice sheet dynamics, a longer-term palaeoceanographic perspective is needed. In this study we aim to investigate the oceanographic conditions off West Greenland during the important period when the ice sheet retreated from western to eastern Disko Bugt, and subsequently into the Isfjord. Specifically we aim to assess the potential link between ice margin retreat and ocean temperatures during this period. We focus on a new marine sediment core, from the shelf southwest of Disko Bugt, spanning the last *c.* 7 ka BP. The coring site is located directly below the flow path of the WGC and is expected to record: i) meltwater influence from the GIS (received along the West Greenland margin and from Disko Bugt; ii) shifts in the relative contribution of the relatively warm/saline Atlantic (Irminger Current) and colder/fresher Polar (East Greenland Current) water masses to the WGC. Paleoenvironmental reconstructions are inferred from benthic foraminiferal assemblage data. We use groupings of Atlantic and Arctic water species as a proxy to identify qualitative changes in bottom water mass properties of the WGC (e.g. Lloyd et al., 2011; Perner et al., 2011). Our marine based reconstructions will provide a high-resolution longer-term Holocene perspective on the paleoceanographic development of Disko Bugt.

(A) Modern environmental setting of Disko Bugt

Disko Bugt is a large marine embayment (40,000 km^2) in central West Greenland (Figure 1). Shallow water depths, varying between 200 and 400 m are typically found, with maximum water depths up to 900 m in Egedesminde Dyb, a deep water trough of glacial origin (Long and Robert, 2003; Roberts and Long, 2005). Jakobshavn Isbræ, one of Greenland's largest outlet glaciers, flows into Disko Bugt and currently drains about 7% of the GIS (Bindshadler, 1984). The present day oceanographic setting of West Greenland is dominated by the WGC, which is formed by a combination of: i) relatively warm and saline Atlantic-sourced water from the Irminger Current (IC), a side branch of the North Atlantic Current (NAC); ii) Polar-sourced cold, low-salinity water from the East Greenland Current (EGC; Buch, 1981); and iii) local meltwater discharge along the SW Greenland coast (Figure 1). The WGC enters Disko Bugt from the southwest and flows northwards exiting primarily through the Vaigat into Baffin Bay. A branch of the WGC is deflected into Baffin Bay west of Disko Island, while the main current continues to flow along West Greenland northward into northern Baffin Bay (Andersen, 1981; Bâcle et al., 2002; Ribergaard et al., 2006). Temperature and salinity data from Disko Bugt (Andersen, 1981; Buch, 1981; Buch et al., 2004; Lloyd et al., 2006; Harff et al., 2007) show that the WGC (3.5–4°C, 34.2–34.4 PSU) forms the bottom waters within the bay. Andersen (1981) found no indications of admixture of deep Baffin Bay waters below 300 m water depth, penetrating into Disko Bugt. Surface waters, however, are influenced by meltwater flux from land, icebergs and the previous season's pack ice, as well as relatively low-salinity polar surface water advected from Baffin Bay. At present, the

Arctic sea-ice edge, formed annually in Baffin Bay between September and March, is found just north of Disko Bugt in spring (Tang et al., 2004) and influences the surface water productivity in the area (e.g. Hansen et al., 1999; Levinsen et al., 2000).

(A) Material and Methods

This study focuses on the composite record of a multi and gravity core obtained from site MSM 343300 (68°28,311'N/ 54°00,119'W Figure 1) southwest of Disko Bugt (cruise MSM05/03 of the *R/V 'Maria S. Merian'*; Harff et al., 2007). The multi core (length: 28.5 cm) and gravity core (total length: 1132 cm, this study focuses only on the depths 0-400 cm) were retrieved from 519 m water depth in Egedesminde Dyb.

Age control is provided by accelerator mass spectrometry AMS^{14}C dates on mollusc shells and benthic foraminifera (Table 1, Figure 2). The chronology of the composite record (last 7 ka BP) is based on 17 AMS ^{14}C dates. The AMS radiocarbon dates were calibrated using the Marine09 (Reimer et al., 2009) calibration curve in CALIB 6.0.2 (Stuiver and Reimer, 1993). Following the results from Lloyd et al. (2011), we applied a marine reservoir age correction ΔR of 140±35 years, which represents the modern ΔR value for the Disko Bugt area.

Foraminiferal analysis was carried out on a standard volume of 5 ml fresh sediment, soaked in deionized water overnight and gently sieved at 63 µm just before counting. Multi core samples were counted at 1-2 cm intervals and gravity core samples at 4 cm intervals. Calcareous and agglutinated foraminifera were counted on a squared picking tray and identified to species level under a stereomicroscope from the wet residue >63 µm to reduce the loss of the more fragile arenaceous species caused by drying out of sediment. The total number of specimens counted per sample ranges from 300 to about 750. The Shannon-Wiener Index (S(H)), a measure of faunal diversity, was calculated separately for the total (S(H)total; Figure 3), the agglutinated (S(H)agglutinated; Figure 4), and the calcareous (S(H)calcareous; Figure 5) assemblage.

Sediment samples (1 cm interval) were wet sieved at the 63 and 200 µm grain size fraction to determine the sand content. The fraction 63-200 µm is used as an approximate measure of the WGC's current strength and sediments deposited in the fraction >200 µm provide indications of ice-rafted debris (IRD) deposited at the coring site. Additionally, counts of IRD (>2 mm) on X-ray images were carried out. The total organic carbon (TOC) of the bulk sediment (2 cm interval) is determined indirectly by subtracting the total inorganic carbon form the total carbon content.

(A) Results

(B) Age model and lithology

Sediments are composed of mottled olive/greenish grey to moderate olive brown organic rich clay with occasional shell fragments and drop stones. The depth-age model was fitted to the calibrated ^{14}C dates using mixed effect modelling (Heegaard et al., 2005). The age model of the multi core is based on linear interpolation between the AMS ^{14}C date at 26.5 cm depth (Table 1) and the modern age of 2007, the sampling year, for the core top (see Lloyd et al., 2011). Figure 2 presents the age model for the last 7.3 ka BP of the gravity core. According to our age model, a gap of *c.* 500 years exists between the multi and gravity core. Loss of the upper sediments is presumably due to the gravity coring technique. The sedimentation rate in the gravity core averages 0.44 cm/yr between 7.3 and 3.5 ka BP, increasing to 0.85 cm /yr between 3.5 and 1 ka BP.

The content of IRD (>2 mm fraction) is low within the core, supported by low values of the >200 µm % fraction throughout the last *c.* 7 ka BP (Figure 2a). The sand content (63-200 µm % fraction) averages about 8% between 7.3 and 7 ka BP, then increases to maximum values between 7 and 6.3 ka BP (averages 25%; Figure 2b). From about 6 ka BP, there is a gradual decrease in the sand content, reaching an average of about 5% after 3.5 ka BP. The TOC content is initially low with an average of ~1% between 7.3 and 5.5 ka BP, then increases gradually, reaching an average of about 2.5% after 2.5 ka BP (Figure 2c). X-ray radiographs (A. Jennings unpublished data) reveal two turbidites in the record, one at ~3 ka BP (199.5-201.5 cm core depth; peak in sand content; 0.5% drop in TOC content) and one at ~5 ka BP (291-296.5 cm core depth). Data from these depths have been excluded from the record and the following discussion.

(B) The benthic foraminiferal assemblage and ecology

Benthic foraminifera were counted from 120 samples from the combined cores. A total of 52 benthic foraminiferal species were identified: 17 agglutinated and 35 calcareous species (see Appendix I for complete faunal list). Both calcareous and agglutinated specimens were well preserved and showed minimal evidence of post mortem (dissolution) changes throughout the core. This is supported by relatively low counts of test linings per sample (Figure 3). Following previous studies on high-resolution sites from the Disko Bugt area (e.g. Lloyd et al., 2011; Perner et al., 2011), we present changes in the total benthic foraminiferal assemblage (agglutinated and calcareous assemblage) along with summary curves of a chilled Atlantic water group (AtlW) and an Arctic water group (AW). These groupings are based on environmental preferences of the species (associated directly or indirectly with salinity and temperature) and are used to identify changes in the relative temperature and salinity of the WGC associated with changes in the respective water mass composition (IC/EGC influence) during the Holocene.

In Table 2, we present a list of species included in the AtlW and AW group along with references supporting species allocations. The AtlW group includes species such as *Islandiella norcrossi* and *Cassidulina reniforme* (calcareous) and *Adercotryma glomerata*, *Reophax pilulifer*, and *Ammoscalaria pseudospiralis* (agglutinated). In the presented study, *I. norcrossi* is the most abundant species of the AtlW group, indicating a relatively strong IC component of the WGC. The highest abundance of this species is associated with a stable salinity during the most ameliorated oceanic conditions of the Holocene. The AW group includes species such as *Cuneata arctica*, *Spiroplectammina biformis*, and *Textularia torquata* (agglutinated) and *Elphidium excavatum* f. *clavata* and *Islandiella helenae* (calcareous). These species are indicative of relatively fresh and cold water mass characteristics (strong EGC component and/or local meltwater influence from the GIS) within the WGC. The total benthic foraminiferal assemblage also contains various productivity indicator species such as *Nonionellina labradorica*, *Globobulimina auriculata arctica*, *Buccella frigida*, *Melonis barleeanus*, *Epistominella vitrea*, *Stainforthia loeblichi*, *Trifarina fluens* and *Pullenia* sp. The occurrence of these species is often related to high productivity at the sea surface, which enhances food supply to the sea floor and the availability of more or less degraded/altered organic matter within the sediments (e.g. Mudie et al., 1984; Caralp, 1989; Polyak and Solheim, 1994; Jennings et al., 2004).

The relative abundance (%) of the dominant agglutinated and calcareous species based on the total assemblage over the last 7.3 ka BP is presented in Figure 3. Based on changes within the total assemblage, along with changes in AtlW and AW groupings, an informal subdivision into three zones (A-C) has been made. The relative abundance (%) of the agglutinated and calcareous fauna is also plotted separately in Figures 4 and 5. Additionally, we provide absolute abundance of the agglutinated and calcareous fauna (plotted as total specimens counted per ml wet sediment) separately in the supplementary section (Figure S1-agglutinated species; Figure S2-calcareous species).

(C) The agglutinated assemblage

Deuterammina ochracea is the most abundant species of the agglutinated assemblage during the last 7.3 ka BP ranging from 40 to 60%. This is a cosmopolitan species that is found widely in Arctic and sub-Arctic environments and provides limited information on paleoenvironmental change within this study. In zone A, from 7.3 to 6.2 ka BP, AW species (e.g. *C. arctica*, *S. biformis*) are relatively common averaging 10% of the fauna. This suggests relatively cold and fresh bottom water mass conditions. At about 6.5 ka BP, there is a slight increase in AtlW taxa (*R. pilulifer*, *S. diflugiformis* and *A. pseudospiralis*, *A. glomerata*), which is possibly linked to occurrence of relatively warmer water masses at that time.

In zone B, *E. advena* increases to 15-20% between 6.2 to 5.6 ka BP, and *Cribrostomoides* sp. averages 10% during this time interval. A minor rise noted in AW species at *c.* 6.3 ka BP suggests a short-term cooling and freshening of bottom water conditions. From *c.* 5.5 to 3.5 ka BP, we find lowest occurrence of the AW group over the period studied, which indicates minimum influence from either local meltwater sources in Disko Bugt or from the EGC component to the WGC during this time interval.

In zone C, from *c.* 1.7 ka BP onwards, we note a gradual rise in overall abundances and diversity of agglutinated specimens (S(H) Index exceeds 1.5). AtlW species (*A. glomerata*, *A. pseudospiralis*, *and S. diflugiformis Reophax* sp.) increase rapidly from *c.* 1.6 ka BP, reaching peak abundance of about 30% (Figure 4). Subsequently, from *c.* 1.6 to 1.3 ka BP, a slight reduction in abundance of this group occurs to about 20%. AW species show a gradual increase from *c.* 1.5 ka BP, reaching peak values of approximately 30% from *c.* 0.9 ka BP onwards indicating subsequent freshening and cooling.

(C) The calcareous assemblage

Between 7.3 and 6.3 ka BP (zone A), AtlW species dominate (40-80%), but co-occurrence with AW species (10-40%) presumably reflects mixed (warm and fresh) bottom water conditions. The overall abundance of productivity indicator species (e.g. *N. labradorica*, *B. frigida*) is relatively low through this interval. Relatively high abundance of *M. barleeanus*, compared to following intervals, suggests that relatively old/degraded organic material is present at the site, with limited replenishment from surface productivity at this time. At *c.* 7 ka BP, peak abundance of the AtlW group (Figure 5; S2) reflects relatively warmer bottom water conditions.

In zone B, peak abundance of *N. labradorica*, centred at 6 ka BP, indicates a prolonged period of high surface water productivity, causing enhanced supply of fresh phytodetritus to the sea floor. A pronounced rise in AW species (e.g. *Elphidium excavatum* f. *clavata*, *I. helenae*) is also noted with peak abundance at *c.* 5.5 ka BP, suggesting possible bottom water cooling. Subsequently, a pronounced decline in the abundance of *E. excavatum* f. *clavata* is noted, coinciding with an increase in AtlW species. From about *c.* 5.5 to 3.5 ka BP, the AtlW group dominates the assemblage, documenting relatively warm and ameliorated bottom water conditions in the area (Figure 5; S2).

In zone C, we observe a rise in AW species, in particular *E. excavatum* f. *clavata*, but also a minor increase in *I. helenae*, reaching a peak at *c.* 2.7 ka BP indicating cooling of bottom water conditions. The abundance of the AtlW group declines through this interval, although a sudden peak in abundance is seen at *c.* 1.8 ka BP, comparable to abundances found between *c.* 5.5 and 3.5 ka BP. This indication of a relatively warm WGC is accompanied by low abundance of AW species (e.g. *E. excavatum* f. *clavata*) at *c.* 1.8 ka BP.

The most prominent feature in the uppermost part of the record is the abrupt decrease of *E. excavatum* f. *clavata*, *I. norcrossi* and *C. reniforme* from about 0.9 ka BP onwards, implying a change to harsher environmental conditions than previously.

(A) Discussion

(B) Long-term Holocene changes in oceanographic variability of the WGC

Our new benthic foraminiferal record, from the shelf southwest of Disko Bugt, illustrates the permanent influence of the WGC, influencing the oceanographic conditions within the area over the last *c.* 7 ka BP. From our data, the grouping of AtlWcalc and AWagg indicator species, we can extract two main factors that influence water mass properties of the WGC over time: i) meltwater influence from the GIS, received along the West Greenland margin and from local sources in the Disko Bugt region; ii) shifts in the relative contribution of warm/saline Atlantic (IC) and of colder/fresher Polar (EGC) water masses to the WGC. The variations in local influence from the GIS and regional ocean forcing will be discussed below.

(C) Meltwater influence from the GIS (7.3 to *c.* 6.2 ka BP) in the Disko Bugt area

Post-glacial reappearance of the WGC is reported from the West Greenland area and the Canadian Arctic already after *c.* 9 ka BP (e.g. Hillaire-Marcel et al., 2001; Lloyd et al., 2005; Knudsen et al., 2008a; Ren et al., 2009; Jennings et al., in prep.). Evidence from marine and terrestrial records suggest that the GIS retreated from the shelf west of Disko Bugt to the eastern part of the embayment by *c.* 10.2 ka

BP (e.g. Long and Roberts, 2002; Long and Roberts, 2003; Lloyd et al., 2005; Young et al., 2011).

Strong melting from the GIS, translated to runoff into the ocean, is reported between 8 and 6 ka BP (Alley and Anandakrishnan, 1995), and is thought to be in response to atmospheric forcing, i.e. pronounced temperature rise over the GIS (Dahl-Jensen et al., 1998; Vinther et al., 2009). In addition to this proposed atmospheric forcing, our reconstructions (zone A) provide evidence of an ocean forcing, with a relatively warm WGC entering Disko Bugt from *c.* 7.3 to 6.3 ka BP, which presumably supportes ice sheet melt in the area. This lower part of the record is also characterized by strong variability in the flow strength of the WGC, displayed by the sand content (Figure 6c). Initially, between 7.3 and 7 ka BP, decreasing sand content suggests a weaker flow of the WGC (Figure 6c). The fauna is dominated by AtlW species, but with variable amounts of AW species, which presumably reflects a mixed (relatively warm and fresh) WGC (Figure 3). A relatively weaker flow of the WGC might be related to meltwater influence from the GIS, received during the travel of the current along the West Greenland margin. This interval coincides also with reduced deposition of biogenic carbon (Figure 6e; MD99-2322) and low abundance of AtlW species on the East Greenland shelf south of Denmark Strait, attributed to continuing and enhanced melting from the GIS (Jennings et al., 2011). Following this initial period, from *c.* 7 ka BP, significant increase in sand content reflects a strengthening of the WGC flow, and a maximum is seen between 6.5 and 6.3 ka BP (Figure 6c). During this period, post-glacial initiation of deep convection is reported from the Labrador Sea (Hillaire-Marcel et al., 2001). The relatively low TOC content and relatively high abundance of *M. barleeanus*, feeding on altered organic matter (e.g. Caralp, 1989), indicates low in situ marine productivity at this time. We postulate that relatively warmer bottom water flow into Disko Bugt supports/enhances ice sheet retreat and caused enhanced meltwater production that circulated within the embayment at this time. In turn, this meltwater discharge influences surface water productivity, which is translated into reduced concentration of foraminiferal tests (Figure 3) and lower abundance of productivity indicator species feeding on fresh phytodetritus (e.g. *N. labradorica*, Figures 5, S2). This influence of surface water productivity is prominently seen, when comparing the relative abundance and concentration (no. of specimens per ml) of the AtlW group (see Figure 3, red and light red graphs).

The increased flow of the WGC, accompanied by a rise in the concentration of the AtlWcalc (Figure 6d) from *c.* 7 ka BP, correlates with enhanced deposition of biogenic carbon and an abrupt rise in AtlW species in a core from the southern Denmark Strait after *c.* 7 ka BP, which Jennings et al. (2011) relate to a warmer and stronger IC (Figure 6e). Our results suggests that meltwater runoff from the GIS started to decline after 7 ka BP and had reduced influence on the water mass composition of the WGC along the West Greenland margin. This is supported by terrestrial reconstructions, which report a largely land-based ice sheet by *c.* 7 ka BP, which had retreated behind its present margin in eastern Disko Bugt (Weidick and Bennike, 2007).

(C) Thermal optimum oceanographic conditions (6.3 to ~3.5 ka BP) in the Disko Bugt area

A significant shift in oceanographic conditions is observed from 6.3 ka BP onwards (zone B). This period starts with a prominent peak in productivity, shown by the dominance of *N. labradorica*, between 6.3 and 5.8 ka BP (Figure 5). This most likely relates to enhanced surface water productivity leading to increased supply of fresh phytodetritus (food supply) to the sea floor. Such a strong productivity event indicates a shift in the time period, when Arctic sea-ice breakup occurs in spring months at Disko Bugt. We assume that prior to *c.* 6 ka BP the Arctic sea-ice edge was positioned further south of Disko Bugt and breakup of the sea-ice edge occurred during summer months at Disko Bugt, causing a greater annual bloom over the core site. This is further supported by the occurrence of *I. helenae* and *S. loeblichi* between 6.3 and 5.5 ka BP (Figure 5; Polyak and Solheim, 1994). From *c.* 5.5 ka BP onwards, the distribution of *N. labradorica* remains at a continuously relatively lower level, suggesting reduced sea-ice edge influence southwest of Disko Bugt.

Geomorphological studies in the eastern Disko Bugt area report a largely land-based ice sheet and reduced meltwater runoff from the GIS after *c.* 6 ka BP (Weidick et al., 1991; Weidick and Bennicke, 2007; Briner et al., 2010). As the ice sheet in the Disko Bugt area was now largely land-based, entrainment of the relatively warm WGC into the embayment could have no direct impact on the ice sheet and force enhanced melting. Consequently, local meltwater discharge from the GIS in the Disko Bugt area will have a more limited influence on the oceanographic record at our core site southwest of Disko Bugt. From this time onwards, the WGC presumably displayed the dominant water mass in Disko Bugt, and it is likely to have influenced surface water properties as well. Henceforth, shifts in abundance of the AtlWcalc and AWagg groups would now indicate changes in the qualitative water mass contributions from the WGCs source currents (EGC and IC, respectively). The overall dominance of the AtlWcalc fauna, between *c.* 5.5 to 3.5 ka BP (Figure 6d), highlights strong contribution from the IC, and hence a relatively warm and saline WGC in Disko Bugt. A strong and relatively warm IC is also reported from the East Greenland shelf (Figure 6e; Jennings et al., 2002; Jennings et al., 2011) and to the south of Iceland during this time interval (e.g. Knudsen et al., 2008b).

Already after 6 ka BP, we observe decreasing current strength of the WGC at the coring site by decreasing sand content to about 15% at 4.0 ka BP (Figure 6c). The reduced flow speed of the WGC registered at the core site does not affect the relative warmth of the WGC, as shown by the dominance and high concentration of the AtlWcalc group at that time (Figure 6d). We assume that the main core of the WGC moved away from the sea floor at the core site. This is accompanied by a slight increase in sedimentation rate, coincident with a increasing TOC (%) content, which is most likely related to enhanced in situ marine productivity at the sea surface (Figures 6a, b).

Between *c.* 5.5 and 3.5 ka BP, we find low abundance of total AW species (e.g. *E. excavatum* f. *clavata*; *C. arctica*, and *S. biformis*; Figures 4, 5, 6f), reflecting minimum influence of cool freshwater either from the GIS meltwater and/or the EGC during this period. Accordingly, regional oceanographic conditions had stabilized between *c.* 5.5 and 3.5 ka BP and the warmest, most ameliorated oceanographic bottom water conditions, reflecting 'thermal optimum-like' conditions prevailed. As noted above, a relatively warm WGC was already present in the area from *c.* 7.3 ka BP onwards, but until *c.* 5.5 ka BP, the regional oceanographic signal was overprinted by the influence of ice sheet meltwater on the WGC at the site.

The faunal data, presented here, tend to support an interpretation of extended 'thermal optimum-like' conditions from *c.* 7 to 3.5 ka BP. The assumption of a longer optimum would be in accordance with previous reconstructions of thermal optimum conditions from terrestrial and marine studies in the Disko Bugt area (Funder and Weidick, 1991; Fredskild, 2000; Lloyd et al., 2007; Young et al., 2011). Relatively late thermal optimum conditions in the bottom waters southwest of Disko Bugt also supports the spatially variable nature of Holocene Thermal Maximum (HTM) conditions, caused by local ice sheet melt influence (see discussion by Kaufman et al., 2004; Kaplan and Wolfe, 2006). Nonetheless, increased occurrence of drift ice on the North Iceland Shelf from 5.5 ka BP onwards (Figure 6g), attributed to an expansion of the EGC, indicates a climatic shift, involving widespread circulation changes in the high latitude North Atlantic (Figure 6g; Moros et al., 2006a). This might consequently also affect the flow strength of the WGC southwest of Disko Bugt.

(C) Onset of Neoglacial cooling (3.5 ka BP to present)

From about 3.5 ka BP onwards (zone C) the benthic foraminiferal assemblage documents cooling/deterioration of the oceanographic/environmental conditions at the core site. We observe cooling/freshening (increase in total abundance of agglutinated specimens and AWagg fauna; Figure 6f) and weakening (decrease in sand content; Figure 6c) of the WGC. This cooling trend is consistent with results from a previous study of nearby coring site 343310 (Figure 1; Perner et al., 2011) and is attributed to an enhanced influence of the EGC. This increased contribution of relatively cold and fresh water masses to the WGC correlates with the onset of Neoglacial cooling in West Greenland.

After 3.5 ka BP, the sedimentation rate increases from an average rate of 0.44 cm/yr to about 0.85 cm/yr, accompanied by a 1% rise in TOC content (Figure 6a, b). This is linked to enhanced in situ productivity at the site, which may also be a consequence of the notably weaker WGC, compared to the preceding intervals (Figure 6c). The observed deterioration of environmental conditions, initiated around 3.5 ka BP, corresponds well with the reported termination of relatively warm conditions on the NW Iceland Shelf (Jiang et al., 2002), in the Denmark Strait (decrease in biogenic carbon content, Figure 6e; Jennings et al., 2011) and in western/south Greenland (e.g. Fredskild, 1984, 2000; Bennike, 2000; Kaplan et al., 2002; Kuijpers et al., 2003; Lassen et al., 2004; Moros et al., 2006b; Møller et al., 2006; Seidenkrantz et al., 2007, 2008; Lloyd et al., 2007). In addition to this oceanic cooling, terrestrial reconstructions suggest an advance of the GIS after 4 ka BP within the Disko Bugt area (Weidick and Bennike, 2007; Briner et al., 2010, Young et al., 2011), as well as cooling over the GIS (Dahl-Jensen et al., 1998), coinciding with decreasing summer solar insolation (Berger and Loutre, 1991).

Superimposed on this late Holocene cooling trend we find multi-centennial scale variability in the WGC, correlating with the variability reported by Perner et al. (2011). A cooling around 2.5 ka BP (increased abundance of AW species *I. helenae*; Figure 5, S2), is associated with the 2.7 ka BP 'cooling event', which has been recorded in various marine and terrestrial records in the North Atlantic region (e.g. Oppo et al., 2003; Risebrobakken et al., 2003; Hall et al., 2004; Moros et al., 2004). A pronounced relatively warm phase is seen at 1.8 ka BP (marked increase in the AtlWcalc fauna; Figure 6d), can be linked to the Roman Warm Period 'RWP'. This period records oceanographic conditions comparable to, or perhaps slightly warmer than the 'thermal optimum-like' conditions seen between *c.* 5.5 and 3.5 ka BP of West Greenland. Significant warming during the 'RWP' also correlates with findings from the Reykjanes Ridge in the central North Atlantic (Moros et al., in press).

The gradual cooling of bottom water conditions, which becomes more pronounced from ~1.8 ka BP onwards (gradual rise in AWagg species; Figure 6f), indicates enhanced freshwater forcing from the EGC (cf. Perner et al., 2011) and reduction in IC contribution to the WGC. Nonetheless, a minor warming of bottom water conditions is seen between 1.4 and 0.9 ka BP (Figure 6d), which corresponds to the 'MCA', suggesting a continuous significant IC contribution to the WGC during this time period. The foraminiferal fauna shows that the 'MCA' warming is less pronounced than that of the 'RWP', and it is also evident that the 'RWP' records the warmest phase during the late Holocene (see Figure 6d; Perner et al., 2011). Relative cooling of oceanographic conditions from the 'RWP' to the 'MCA', between 1.8 and 0.7 ka BP, agrees well with previous findings from the Disko Bugt area (Perner et al., 2011) and with other marine records from the northern North Atlantic (e.g. Andrews and Giraudeau, 2003; Moros et al., 2004, 2006a, in press; Richter et al., 2009).

No sediments are recovered in the present record between 0.7 and 0.3 ka BP (gap in composite record of core 343300). However, severe cooling is seen after 0.9 ka BP culminating in the 'Little Ice Age' at 0.3 ka BP related to a continuous increase in the EGC component of the WGC (rise in overall abundance/diversity of agglutinated species and the AWagg fauna, Figure 6f, and supplemented with data from core 343310 (Perner et al., 2011); Figure 6d – light red line, 6f – light blue line). Enhanced EGC contribution to the WGC during the 'LIA' is supported by studies from the East Greenland Shelf, North Icelandic Shelf, Denmark Strait and Southeast and West Greenland, reporting expansion and intensification of the EGC by enhanced contribution of relatively fresher/colder Polar water masses and increased drift ice (e.g. Figure 6g) within the EGC (Andrews et al., 1997; Kuijpers et al., 2003; Eiríksson et al., 2004; Moros et al., 2006a; Jennings et al., 2011; Sha et al., 2011). This oceanic cooling encompasses the reported re-advance of Jakobshavn Isbræ, to its LIA maximum position, 20 km west of its current position (Weidick et al., 1990).

Reconstructions by Kaufman et al. (2009) from terrestrial archives document a strong increase in arctic summer air temperature during the last *c.* 100 years. Contrary to this our data show that oceanographic conditions (WGC) are relatively cool and remained cooler during the last 100 years than during the 'MCA'. Similar results were obtained by Sha et al. (2011) from a site further south on the West Greenland Shelf. These environmental conditions are presumably determined by a relatively strong contribution from the cold EGC during the last 100 years, and are in agreement with the freshening of Baffin Bay between 1916-2003, reported by Zweng and Münchow (2006).

(A) Summary and Conclusions

A new Holocene benthic foraminiferal record from southwest Disko Bugt provides detailed information of multi-centennial scale bottom water (WGC) variability off West Greenland and interaction of the WGC with the West Greenland ice sheet. Our reconstructions provide a long-term Holocene perspective on the influence of ocean forcing on the Greenland Ice Sheet in the Disko Bugt area.

Between *c.* 7 and 6.3 ka, we observe, a relatively warm and strong WGC, which is likely to support ice sheet melt in Disko Bugt, leading to increased meltwater production, and consequently results in low surface water productivity. A subsequent strong productivity event at *c.* 6 ka BP suggests that the Baffin Bay Arctic sea-ice edge migrated from its location to the south of Disko Bugt northwards across the site, presumably linked to the influence of the relatively warm and strong WGC. A prolonged relatively warm/stable phase of the WGC is indicated by persisting dominance of the AtlWcalc fauna from *c.* 5.5 to 3.5 ka BP, reflecting 'thermal optimum-like' conditions off West Greenland.

Most likely a relatively warm and strong WGC was continuously present on the shelf of Disko Bugt during the entire period between *c.* 7 and 3.5 ka BP, albeit its signal is diluted/deflected (overprinted) in our data by the melting ice sheet, which in turn resulted in relatively cooler and variable environmental conditions.

From about 3.5 ka BP, benthic foraminifera identify a long-term late Holocene cooling of the bottom waters, associated with the onset of Neoglacial cooling. This indication of a long-term cooling agrees well with studies from West/East Greenland fjord and shelf areas, which report gradual cooling of the WGC, along glacial re-advances. It is likely that cooling of oceanographic conditions favoured the observed re-advance of the ice sheet in the Disko Bugt area after c. 3.5 ka BP. Superimposed on this cooling trend, we reconstruct marked multi-centennial scale variability within the WGC: i) a cooling at *c.* 2.5 ka BP, related to the 2.7 ka BP ‘cooling event’; ii) a relatively warm phase at *c.* 1.8 ka BP, corresponding to the ‘Roman Warm Period’; iii) only a slight warming in bottom waters at the transition into the ‘Medieval Climate Anomaly’ and; iv) strong cooling from *c.* 1.8 ka BP culminating in the ‘Little Ice Age’ cold period.

Cooling of bottom waters, confirmed by a gradual rise in AWagg species, is linked to an enhanced influence of fresher/cooler water mass contribution from the EGC to the WGC. Agglutinated species dominate the benthic foraminiferal assemblage also during the last 100 years, corroborating a persistent strong influence of the EGC on the WGC, consistent with previous studies from Disko Bugt and the West Greenland shelf.

Acknowledgements

The authors thank the Deutsche Forschungsgemeinschaft (DFG) for funding the project ‘Disko Climate’ (MO1422/2-1). We also thank the Captain and Crew of the R/V ‘Maria S. Merian’ for their fantastic work during cruise MSM05/03. We thank Marit-Solveig Seidenkrantz for fruitful discussion of the benthic foraminiferal assemblage and their interpretation, Tomasz Goslar from Poznań Radiocarbon Laboratory and also Richard Telford from the University of Bergen, for performing the age-depth modelling of the gravity core.

(A) References

Alley RB, Anandakrishnan S (1995) Variations in melt-layer frequency in the GISP2 ice core: implications for the Holocene summer temperatures in central Greenland. *Glaciology* 21: 64-70.

Andersen OGN (1981) The annual cycle of temperature, salinity, currents and water masses in Disko Bugt and adjacent waters, West Greenland. *Meddelelserom Grønland, Bioscience* 5: 1-36.

Andrews JT, Smith LM, Preston R, Cooper T, Jennings AE (1997) Spatial and temporal patterns of iceberg rafting (IRD) along the east Greenland margin, ca.68 N, over the last 14 cal. ka. *Journal of Quaternary Science* 12: 1-13.

Andrews JT, Giraudeau J (2003) Multi-proxy records showing significant Holocene environmental variability: the inner N. Iceland shelf (Hunafloi). *Quaternary Science Reviews* 22: 175-193.

Bâcle JE, Carmack C, Ingram RG (2002) Water column structure and circulation in the North Water during spring transition: April-July 1998.*Deep Sea Research* 49: 4907-4925.

Bennike O (2004) Holocene sea-ice variations in Greenland: onshore evidence. *The Holocene* 14: 607-613

Berger A, Loutre MF (1991) Insolation values of the climate of the last 10 million years. *Quaternary Science Reviews* 10: 297-318

Bindschadler RA (1984) Jakobshavns Glacier drainage basin; a balance assessment. *Journal of Geophysical Research. C. Oceans and Atmospheres* 89: 2066-2072.

Bindschadler R (2006) Hitting the Ice Sheets Where It Hurts. *Science* 311:1720-1721

Buch E (1981) A Review of the oceanographic conditions in subarea O and 1 in the decade 1970- 79. NAFO Symposium on Environmental conditions in the Northwest Atlantic during 1970-79. NAFO Scientific Council Studies no.5.

Buch E, Pedersen SA, Ribergaard MH (2004) Ecosystem Variability in West Greenland Waters. *Journal of Northw. Atl. Fish. Sci.*34: 13-28.

Briner JP, Stewart HAM, Young NE, Philipps W, Losee S (2010) Using proglacial-threshold lakes to constrain fluctuations of the Jakobshavn Isbræ ice margin, western Greenland, during the Holocene. *Quaternary Science Reviews* 29: 3861-3874.

Caralp MH (1989) Abundance of *Bulimina exilis* and *Melonis barleeanum*: Relationship to the quality of marine organic matter. *Geo-Marine Letters* 9:37-43.

Dahl-Jensen D, Mosegaard K, Gundestrup N, Clow GD, Johnsen SJ, Hansen AW, Balling N (1998) Past temperatures directly from the Greenland Ice Sheet. *Science* 282: 268-271.

Duplessy JC, Invanova EV, Murdmaa IO, Paterne M, Labyrie L (2001) Holocene palaeoceanography of the northern Barents Sea and variations of the northward heat transport by the Atlantic Ocean. *Boreas* 30: 2-16.

Eiríksson J, Larsen G, Knudsen KL, Haflidason H, Heinemeier J,Simonarson LA (2004) Marine reservoir age variability and water mass distribution in the Iceland Sea. *Quaternary Science Reviews* 23: 2247-2268.

Fredskild B (2000) The Holocene vegetational changes on Qeqertarsuatsiaq, a west Greenland island. *GeografiskTidsskrift* 100: 7-14.

Funder S, Weidick A (1991) Holocene boreal molluscs in Greenland – palaeoceanographic implications. *Palaeogeography, Palaeoclimatology, Palaeoecology* 85: 123-35.

Funder S, Kjeldsen KK, Kjær, KH, Ó Cofaigh C (2011) The Greenland Ice Sheet

During the Past 300,000 Years: A Review. In J. Ehlers, Gibbard PL and Hughes PD, editors: *Developments in Quaternary Science* 15, Amsterdam, The Netherlands; 699-713.

Hald M, Steinsund PI (1996) Benthic foraminifera and carbonate dissolution in surface sediments of the Barents- and Kara Seas. *Berichte zur Polarforschung* 21: 996.

Hald M, Korsun S (1997) Distribution of modern benthic foraminifera from fjords of Svalbard, European Arctic. *Journal of Foraminiferal Research* 27: 101-122.

Hall IG, Bianchi G, Evans JR (2004) Centennial to millennial scale Holocene climate-deep water linkages in the North Atlantic. *Quaternary Science Reviews* 23, 1529-1536.

Hansen BW, Nielsen TG, Levinsen H (1999) Plankton community structure and carbon cycling on the western coast of Greenland during the stratified summer situation. III. Mesozooplankton. *Aquatic Microbial Ecology* 16: 233-249.

Harff J, Dietrich R, Endler R, Hentzsch B, Jensen J B, Kuijpers A, Krauss N, Leipe T, Lloyd JM, Mikkelsen N, Moros M, Perner K, Richter A, Risgaard-Petersen N, Rysgaard S, Richter T, Sandgren P, Sheshenko V, Snowball I, Waniek J, Weinrebe W, Witkowski A (2007) Deglaciation history, coastal development, and environmental change during the Holocene in western Greenland. *Cruise report R/V Maria S. Merian, cruise MSM 05/03.*

Heegaard E, Birks HJB, Telford JT (2005) Relationships between calibrated ages and depth in straigraphical sequences: an estimation procedure by mixed effect regression. *The Holocene* 15: 612-618.

Hillaire-Marcel C, de Vernal A, Bilodeau G, Weaver A (2001) Absence of

Deepwater formation in the Labrador Sea during the last interglacial period. *Nature* 410: 1073-1077.

Hogan K, Dix J, Lloyd J, Long A, Cotterill C (2011) Near surface stratigraphy of eastern Disko Bugt, West Greenland: implications for glacimarine sedimentation. *Journal of Quaternary Science* 26, 757-766.

Holland DM, Thomas RH, De Young B, Ribergaard MH, Lyberth B (2008) Acceleration of Jakobshavn Isbrae triggered by warm subsurface ocean waters*. Nature Geoscience* 1: 659-664.

Howat IM, Joughin I, Scambos TA (2007) Rapid changes in ice discharge from Greenland outlet glaciers. Science 315: 1559-1561.

Howat IM, Joughin I, Fahnestock M, Smith BE, Scambos TA (2008) Synchronous retreat and acceleration of southeast Greenland glaciers 2000-06: ice dynamics and coupling to climate. *Journal of Glaciology* 54: 646-660.

Ishman SE, Foley KM (1996) Modern benthic foraminifer distribution in the Amerasian Basin, Arctic Ocean. *Micropaleontology* 42: 206-220.

Jakobsson M, Macnab R, Mayer L, Anderson R, Edwards M, Hatzky J, Schenke HW, Johnson P (2008). An improved bathymetric portrayal of the Arctic Ocean: implications for ocean modeling and geological, geophysical and oceanographic analyses. *Geophysical Research Letters* 35, L07602. doi:10.1029/2008GL033520.

Jennings AE, Helgadóttir G (1994) Foraminiferal assemblages from the fjords and shelf of eastern Greenland. *Journal of Foraminiferal Research* 24: 123-44.

Jennings AE, Hagen S, Hardardottir J, Stein R, Ogilvie AEJ, Jonsdóttir I (2001) Oceanographic change and terrestrial human impacts in a post A.D. 1400 sediment record from the southwest Iceland shelf. *Climatic Change* 48 (Special Issue, The Iceberg in the Mist: Northern Research in Pursuit of ‘A Little Ice Age’, guest editors Ogilive AE and Jónsson T), 83-100.

Jennings AE, Knudsen KL, Hald M, Hansen CV, Andrews JT (2002) A mid-Holocene shift in Arctic sea-ice variability on the East Greenland Shelf. *The Holocene* 12: 49-58.

Jennings AE, Weiner NJ, Helgadottir G, Andrews JT (2004) Modern foraminiferal faunas of the southwestern to northern Iceland shelf: oceanographic and environmental controls. *Journal of Foraminiferal Research* 34, 180-207.

Jennings AE, Andrews J, Wilson L (2011) Holocene environmental evolution of the SE Greenland Shelf North and South of the Denmark Strait: Irminger and East Greenland current interactions. *Quaternary Science Reviews* 30: 980-998.

Jennings AE, Perner K, Moros M, Walton M, Andrews JT, Ó Cofaigh C, in prep. Holocene paleoenvironments and deglaciationhistory of SW Disko Bugt based on multi proxy analyses. *In preparation for Journal of Quaternary Science.*

Jiang H, Seidenkrantz MS, Knudsen KL, Eiríksson J (2002) Late-Holocene summer sea surface temperatures based on a diatom record from the north Icelandic shelf. *The Holocene* 12: 137-147.

Joughin I, Abdalati W, Fahnestock M (2004) Large fluctuations in speed on Greenland’s Jakobshavn Isbræ glacier. *Nature* 432: 608-610.

Joughin I, Das SB, King MA, Smith BE, Howat IM, Moon T (2008) Seasonal speed up along the western flank of the Greenland Ice Sheet. *Science* 320: 781–783.

Kaplan MR, Wolfe AP, Miller GH (2002) Holocene environmental variability in southern Greenland inferred from lake sediments. *Quaternary Research* 58: 149-159.

Kaplan MR, Wolfe AP (2006) Spatial and temporal variability of Holocene temperature trends in the North Atlantic sector. *Quaternary Research* 65: 223-231.

Kaufman DS, Ager TA, Anderson NJ, Anderson PM, Andrews JT, Bartlein PJ, Brubaker LB, Coats LL, Cwynar LC, Duvall ML, Dyke AS, Edwards ME, Eisner WR, Gajewski K, Geirsdóttir A, Hu FS, Jennings AE, Kaplan MR, Kerwin MW, Lozhkin AV, MacDonald GM, Miller GH, Mock CJ, Oswald WW, Otto-Bliesner BL, Porinchu DF, Rühland K, Smol JP, Steig EJ, Wolfe BB (2004) Holocene thermal maximum in the western Arctic (0–180°W). *Quaternary Science Reviews* 23: 529-560.

Kaufman DS, Schneider DP, McKay NP, Ammann CA, Bradley RS, Briffa KR, Miller GH, Otto-Bliesner BL, Overpeck JT, Vinther BM, Arctic Lakes 2k Project Members (2009) Recent warming reverses long-term Arctic cooling. *Science* 325: 1236-1239.

Knudsen KL, Seidenkrantz MS (1994) *Stainforthia feylingi* new species from artic to subartic environments, previously recorded as *Stainforthia schreibersiana* (Czjzek). *Cushman Foundation for Foraminiferal Research Special Publication* 32: 5-13.

Knudsen KL, Stabell B, Seidenkrantz MS, Eiríksson J, Blake Jr W (2008a) Deglacial and Holocene conditions in northernmost Baffin Bay: sediments, foraminifera, diatoms and stable isotopes. *Boreas* 37: 346-376.

Knudsen KL, Søndergaard MKB, Eiríksson J, Jiang H (2008b) Holocene thermal maximum off North Iceland: Evidence from benthic and planktonic foraminifera in the 8600-5200 cal year BP time slice. *Marine Micropaleontology* 67: 120-142.

Krawczyk D, Witkowski A, Moros M, Lloyd JM, Kuijpers A, Kierzek A (2010) Late-Holocene diatom-inferred reconstruction of temperature variations of the West Greenland Current from Disko Bugt, central West Greenland. *The Holocene* 20: 659-666.

Kuijpers A, Troelstra SR, Prins MA, Linthout K, Akhmetzhanov A, Bouryak S, Bachmann MF, Lassen S, Rasmussen S, Jensen JB (2003) Late quaternary sedimentary processes and ocean circulation changes at the Southeast Greenland margin. *Marine Geology* 195: 109-129.

Lassen SJ, Kuijpers A, Kunzendorf H, Hoffman-Wieck G, Mikkelsen N, Konradi P (2004) Late-Holocene Atlantic bottom water variability in Igaliku Fjord, South Greenland, reconstructed from foraminifera faunas. *The Holocene* 14: 165-171.

Levinsen H, Turner JT, Nielsen TG, Hansen BW (2000) On the trophic coupling between protists and copepods in arctic marine ecosystems. *Marine Ecology Progress Series* 204:65-77.

Lloyd JM, Park LA, Kuijpers A, Moros M (2005) Early Holocene palaeoceanography and deglacial chronology of Disko Bugt, West Greenland. *Quaternary Science Reviews* 24: 1741-1755.

Lloyd JM (2006) Modern distribution of benthic foraminifera from Disko Bugt, west Greenland. *Journal of Foraminiferal Research* 36: 315-331.

Lloyd JM, Kuijpers A, Long A, Moros M, Park LA (2007) Foraminiferal reconstruction of mid- to late-Holocene ocean circulation and climate variability in Disko Bugt, West Greenland. *The Holocene* 17:1079-1091.

Lloyd JM, Moros M, Perner K, Telford R, Kuijpers A, Jansen E, McCarthy DJ (2011) A 100 year record of ocean temperature control on the stability of Jakobshavn Isbrae, West Greenland. *Geology* 39: 867-870.

Long AJ, Roberts DH (2002) A revised chronology for the 'Fjord Stade' moraine in Disko Bugt, west Greenland. *Journal of Quaternary Science* 17: 561-579.

Long AJ, Roberts DH (2003) Late Weichselian deglacial history of Disko Bugt, West Greenland, and the dynamics of the Jakobshavns Isbrae ice stream. *Boreas* 32: 208-226.

Moon T, Joughin I (2008) Changes in ice front position on Greenland's outlet glaciers from 1992 to 2007. *Journal of Geophysical Research-Earth Surface* 113 F02022, doi: 10.1029/2007JF000927.

Moros M, Emeis K, Risebrobakken B, Snowball I, Kuijpers A, McManus J, Jansen E (2004) Sea surface temperatures and ice rafting in the Holocene North Atlantic: climate influences on northern Europe and Greenland. *Quaternary Science Reviews* 23: 2113-2126.

Moros M, Andrews JT, Eberl DD, Jansen E (2006a) Holocene history of drift ice in the northern North Atlantic: Evidence for different spatial and temporal modes. *Paleoceanography* 21: doi:10.1029/2005PA001214.

Moros M, Jensen KG, Kuijpers A (2006b) Mid- to late- Holocene hydrological and climatic variability in Disko Bugt, central West Greenland. *The Holocene* 16: 357–367.

Moros M, Jansen E, Oppo D, Giraudeau J, Kuijpers A. Reconstruction of the late Holocene changes in the Sub-Arctic Front position at the Reykjanes Ridge, north Atlantic. *The Holocene* (in press).

Møller HS, Jensen KG, Kuijpers A, Aagaard-Sorensen S, Seidenkrantz M-S, Prins M, Endler R, Mikkelsen N (2006) Late-Holocene environment and climate changes in Ameralik Fjord, southwest Greenland: evidence from the sedimentary record. *The Holocene* 16: 685-695.

Mudie P J, Keen CE, Hardy IA, Vilks G (1984) Multivariate-analysis and quantitative paleoecology of benthic foraminifera in surface and late Quaternary shelf sediments, northern Canada. *Marine Micropaleontology* 8: 283-313.

Murray JW (1991) *Ecology and palaeoecology of benthic foraminifera*. London: Longman.

Oppo DW, McManus JF, Cullen JR (2003) Palaeoceanography: deepwater variability in the Holocene epoch. *Nature* 422: 277-278.

Osterman LE, Nelson AR (1989) Latest Quaternary and Holocene paleoceanography of the eastern Baffin Island continental shelf, Canada: benthic foraminiferal evidence. *Canadian Journal of Earth Science* 26: 2236-2248.

Perner K, Moros M, Lloyd JM, Kuijpers A, Telford RJ, Harff J (2011) Centennial scale benthic foraminiferal record of late Holocene oceanographic variability in Disko Bugt, West Greenland. *Quaternary Science Reviews* 30: 2815-2826.

Polyak L, Solheim A (1994) Late- and postglacial environments in the northern Barents Sea, west of Franz Josef Land. *Polar Research* 13: 197-207.

Ren J, Jiang H, Seidenkrantz MS, Kuijpers A (2009) A diatom-based reconstruction of Early Holocene hydrography and climatic change in a southwest Greenland fjord. *Marine Micropaleontology* 70: 166-176.

Reimer PJ, Baillie MGL, Bard E, Bayliss A, Beck JW, Blackwell PG, Bronk Ramsey C, Buck CE, Burr GS, Edwards RL, Friedrich M, Grootes PM, Guilderson TP, Hajdas I, Heaton TJ, Hogg AG, Hughen KA, Kaiser KF, Kromer B, McCormac FG, Manning SW, Reimer RW, Richards DA, Southon JR, Talamo S, Turney

CSM, van der Plicht J, Weyhenmeyer CE (2009) IntCal09 and Marine09 radiocarbon age calibration curves, 0-50,000 years cal BP. *Radiocarbon* 51: 1111-1150.

Ribeiro S, Moros M, Ellegaard M, Kuijpers A (2012) Climate variability in West Greenland during the past 1500 years: evidence from a high-resolution marine palynological record from Disko Bay. Boreas 41: 68-83.

Ribergaard MH, Kliem N, Jespersen M (2006) HYCOM for the North Atlantic Ocean with special emphasis on West Greenland Water. *Technical Report 06-0*. www.dmi.dk/dmi/tr06-07

Richter TO, Peeters FCJ, van Weering T (2009) Late Holocene (0–2.4 ka BP) surface water temperature and salinity variability, Feni Drift, NE Atlantic Ocean. *Quaternary Science Reviews* 28: 1941–1955.

Rignot E, Kanagaratnam P (2006) Changes in the velocity structure of the Greenland Ice Sheet. *Science* 11: 986–990.

Rignot E, Koppes M, Velicogna I (2010) Rapid submarine melting of the calving faces of West Greenland glaciers. *Nature Geoscience* 3:187-191.

Risebrobakken B, Jansen E, Andersson C, Mjelde E, Hevroy K (2003) A high-resolution study of Holocene paleoclimatic and paleoceanographic changes in the Nordic Seas. *Paleoceanography* 18, 1017-1031. doi:10.1029/2002PA000764

Roberts DH, Long AJ (2005) Streamlined bedrock terrain and fast ice flow, Jakobshavns Isbrae, West Greenland: implications for ice stream and ice sheet dynamics. *Boreas* 34: 25-42.

Rytter F, Knudsen KL, Seidenkrantz MS, Eiríksson J (2002) Modern distribution of benthic foraminifera on the North Icelandic shelf and slope. *Journal of Foraminiferal Research* 32: 217-244.

Seidenkrantz MS, Aagaard-Sørensen S, Sulsbrück S, Kuijpers A, Jansen KG, Kunzendorf H (2007) Hydrography and climate of the last 4400 years in a SW Greenland fjord – implications for Labrador Sea palaeoceanography.*The Holocene* 17: 387-401.

Seidenkrantz MS, Roncaglia L, Fischel A, Heilmann-Clausen C, Kuijpers A, Moros M (2008) Variable North Atlantic seesaw patterns documented by a late Holocene marine record from Disko Bugt, West Greenland. *Marine Micropaleontology* 68: 66-83.

Sejrup HP, Birks HJB, Klitgaard-Kristensen D, Madsen H (2004) Benthonic foraminiferal distributions and quantitative transfer functions for the northwest European continental margin. *Marine Micropaleontology* 53: 197-226.

Sha L, Jiang H, Knudsen KL (2011) Diatom evidence of climatic change in Holsteinsborg Dyb, west of Greenland, during the last 1200 years. *The Holocene* 22: 347-358.

Steinsund PI, Polyak LV, Hald M, Mikhailov V, Korsun S (1994) Distribution of calcareous benthic foraminifera in recent sediments of the Barents and Kara Sea. In Steinsund PI, Benthic foraminifera in surface sediments of the Barents and Kara Seas: modern and late Quaternary application. Ph.D. thesis, Department of Geology, Institute of Biology and Geology, Univeristy of Tromsø.

Straneo F, Hamilton GS, Sutherland DA, Staerns LA, Davidson F, Hammill MO, Stenson GB, Rosing-Asvid A (2010). Rapid circulation of warm subtropical waters in a major glacial fjord in East Greenland. *Nature Geoscience* 3: 182–186.

Stuiver M, Reimer PJ (1993) CALIB Radiocarbon calibration program. *Radiocarbon* 35: 215-230.

Tang CCL, Ross CK, Yao T, Petrie B., De Tracey BM, Dunlap E (2004) The circulation, water mass and sea-ice of Baffin Bay. *Progress in Oceanography* 63: 183-228.

Thomas RH (2004) Force-perturbation analysis of recent thinning and acceleration of Jakobshavn Isbræ, Greenland. *Journal of Glaciology* 50: 57-66.

Vilks G (1980) Postglacial basin sedimentation on the Labrador Shelf. *Geological Society of Canada*; 1-28.

Vilks G (1981) Late glacial–postglacial foraminiferal boundary in sediments of eastern Canada, Denmark and Norway. *Geoscience Canadian* 8: 48-56.

Vilks G, Deonarine B (1988) Labrador shelf benthic foraminifera and stable oxygen isotopes of Cibicides lobatulus related to the Labrador Current. *Canadian Journal of Earth Science* 25: 1240-1255.

Vinther BL, Buchardt SL, Clausen HB, Dahl-Jensen D Johnsen S J, Fisher DA, Koerner RM, Raynaud D, Lipenkov V, Andersen KK, Blunier T, Rasmussen SO, Steffensen JP, Svensson AM (2009) Holocene thinning of the Greenland ice sheet. *Nature* 461: 385-388.

Weidick A, Oerter H, Reeh N, Thomsen HH, Thorning L **(**1990) The recession of the Inland Ice margin during the Holocene climatic optimum in the Jakobshavn Isfjord area of West Greenland. Palaeogeography, Palaeoclimatology, Palaeoecology 82, 389–399.

Weidick A, Bennike O (2007) Quaternary glaciations history and glaciology of Jakobshavn Isbræ and the Disko Bugt region, West Greenland: a review. *Geological Survey of Denmark and Greenland Bulletin* 14: 78pp.

Williamson MA, Keen CE, Mudie PJ (1984) Foraminiferal distribution on the continental margin off Nova Scotia. *Marine Micropaleontology* 9: 219–239.

Wollenburg J, Knies J, Machensen A (2004) High-resolution palaeoproductivity fluctuations during the last 24 kyr indicated by benthic foraminifera in the marginal Arctic Ocean: 246. *Palaeogeography, Palaeoclimatology, Palaeoecology* 204: 209-238.

Young NE, Briner, JP, Stewart HAM, Axford Y, Csatho B, Rood DH, Rinkel RC (2011) Response of Jakobshavn Isbræ, Greenland, to Holocene climate change. *Geology* 39: 131-134.

Zarudzki EFK (1980) Interpretation of shallow seismic profiles over the continental shelf in West Greenland between latitudes 64° and 69° 30' N. *Geological Survey of Greenland Report* 100: 58-61.

Zwally HJ, Abdalati W, Herring T, Larson K, Saba J, Steffen K (2002) Surface melt-induced acceleration of Greenland ice-sheet flow. *Science* 297: 218–222.

Zweng MM, Münchow A (2006) Warming and freshening of Baffin Bay, 1916-2003. *Journal of Geophysical Research* 111: C07016, doi:10.1029/2005JC003093.

Figure captions

Figure 1: Schematic bathymetric map of Disko Bugt, adapted from Jakobsson et al. (2008), showing the location of core 343300 (red dot) and 343310 (black star) in south-western Egedesminde Dyb and present day oceanographic setting of the study area. The insert shows schematically the oceanographic setting around Greenland. Abbreviations are as follow: EGC - East Greenland Current; IC – Irminger Current; WGC – West Greenland Current; LC – Labrador Current.

Figure 2: **Lithological characterization and age-depth model of gravity core 343300.** Sediments deposited in the >200 µm fraction (%), number of counted ice-rafted detritus (IRD) >2 mm, the 63-200 µm fraction (%), total organic carbon content (TOC %) and depths of the AMS radiocarbon dates are presented. The age-depth model of the gravity core 343300 is based on linear interpolation between the respective radiocarbon dates. AMS ^{14}C dates are calibrated with the Marine09 (Reimer et al., 2009) calibration curve using Calib602 (Stuiver and Reimer, 1993). For AMS ^{14}C dates, see Table 1.

Figure 3: **Total foraminiferal assemblage (calcareous and agglutinated) from site 343310 versus age.** Foraminiferal frequencies are expressed as a percentage of the total specimens counted. Only species with abundance greater than 10% are included. Additionally, the total number of benthic foraminifera counted, number of benthic foraminifera counted per ml wet sediment, the ratio of calcareous vs. agglutinated specimens, number of test linings and grouping of AtlW (red color) and AW (blue color) indicator species, are presented. The light blue (AW) and light red (Atlw) colored plots show the foraminiferal concentration (no. of specimens per ml wet sediment) of the respective groups. Additionally, we present the Shannon-Wiener-Index (S(H)) calculated for the total benthic foraminiferal assemblage.

Figure 4: **Agglutinated foraminiferal assemblage from site 343300 versus age.** Foraminiferal frequencies are expressed as a percentage of total agglutinated specimens counted. Only species with abundance greater than 2% are included. Red (blue) colored species are included in the AtlW (AW) group. In addition, the Shannon-Wiener-Index (S(H)) was calculated based on the agglutinated fauna.

Figure 5: **Calcareous foraminiferal assemblage of site 343300.** Foraminiferal frequencies are expressed as a percentage of total calcareous specimens counted. Only species with abundance greater than 2% are included. Red (blue) colored species are included in the AtlW (AW) group. In addition, the Shannon-Wiener-Index (S(H)) was calculated based on the calcareous fauna.

Figure 6: **Summary of results compared with other regional data sets.** a) TOC (%) content (343300); b) AMS^{14}C dates against depth (cm, 343300); c) Sand content (% fraction >63-200 µm; 343300); d) number of calcareous Atlantic water specimens (AtlWcalc) per ml wet sediment, red line displays data from site 343300 and light red line data from nearby site 343310; e) Biogenic carbon (%) content of sediments from site MD99-2322, Denmark Strait (Jennings et al., 2011); f) number of agglutinated Arctic water species (AWagg) per ml wet sediment, blue line displays data from site 343300 and light blue line data from nearby site 343310; g) Drift ice proxy data (Quartz%) from core site MD99-2269, NW Iceland (Moros et al., 2006a). Known historical climatic events such as the Roman Warm Period (RWP), the Medieval Climate Anomaly (MCA) and the Little Ice Age (LIA) are marked. The black arrows indicate the position of the two turbidites found in the sediments based on X-ray-radiographs (A. Jennings, unpublished data).

Figure 1

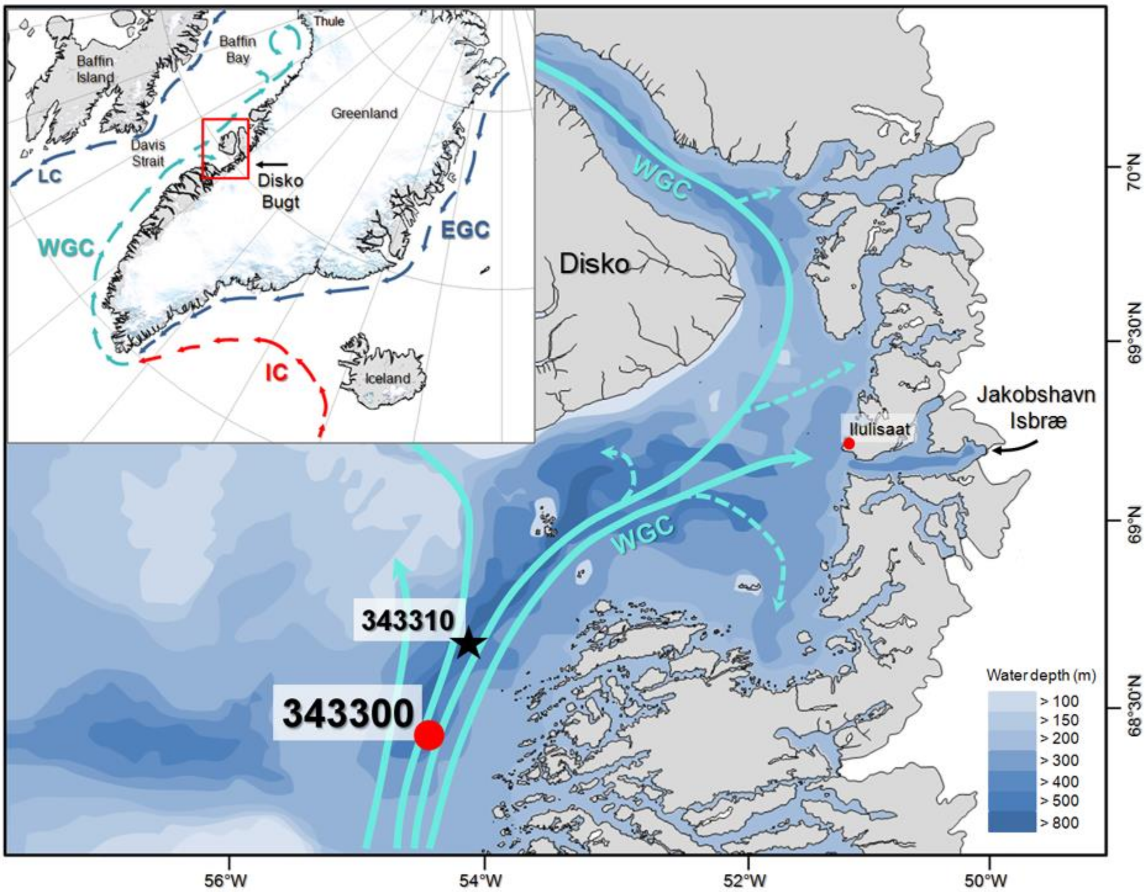

Figure 2

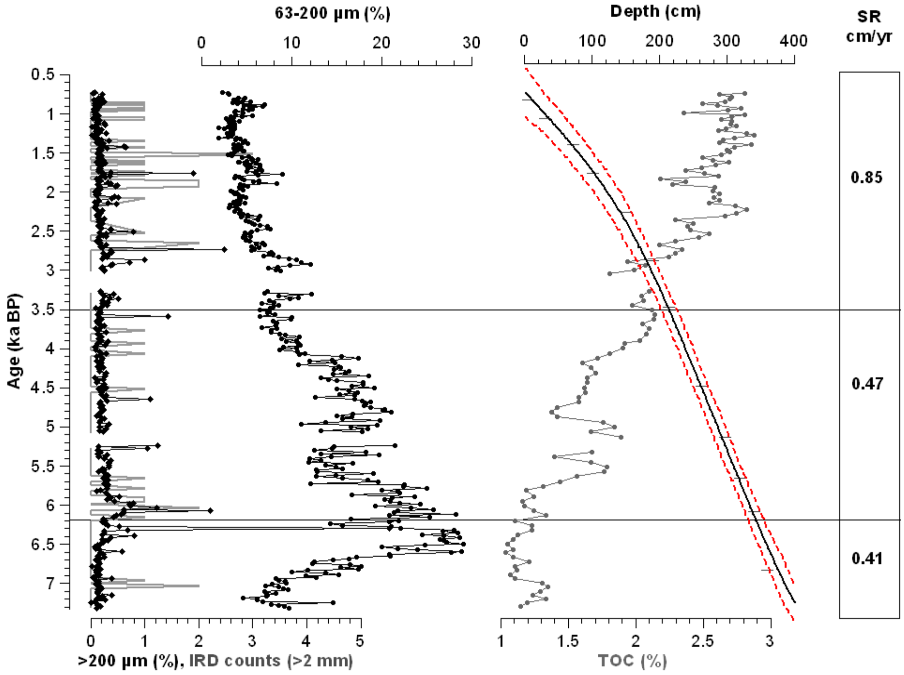

Figure 3

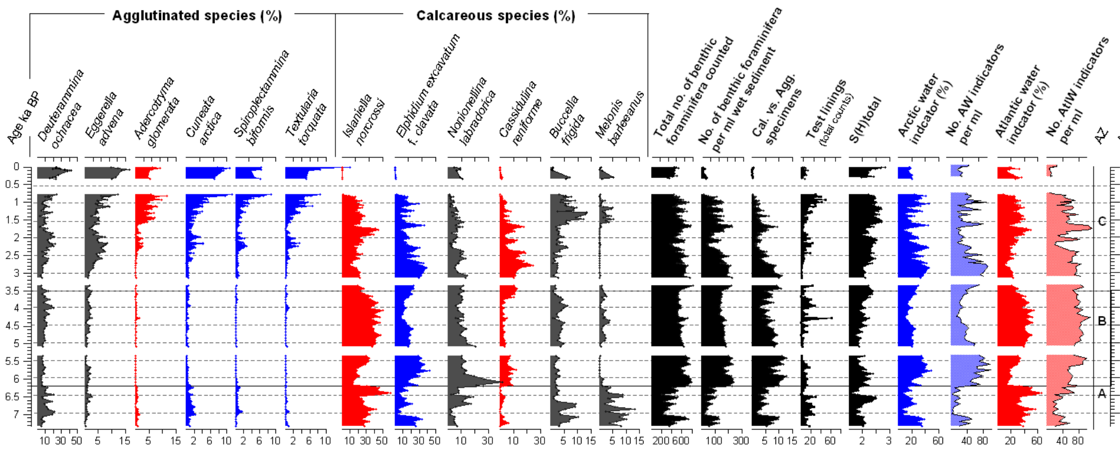

Figure 4

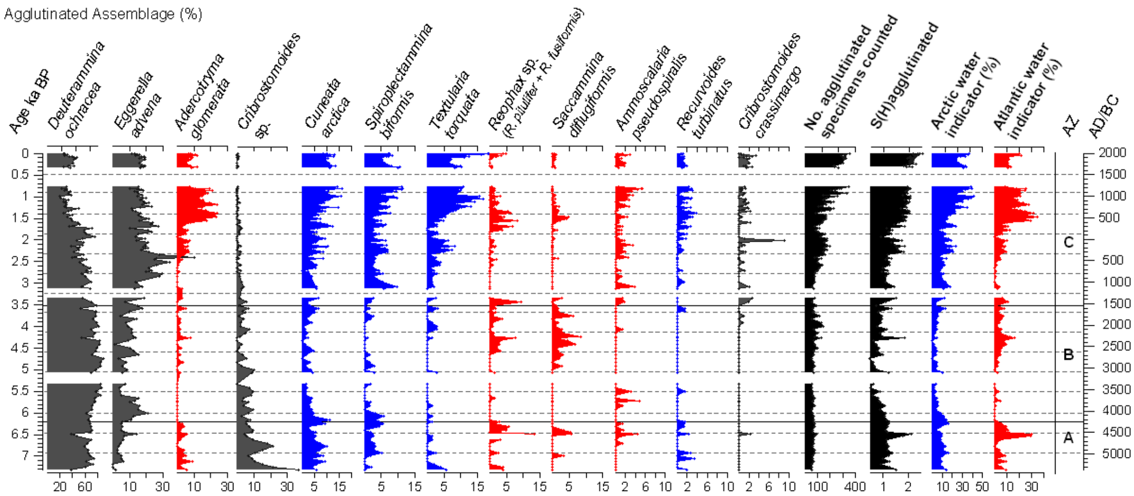

Figure 5

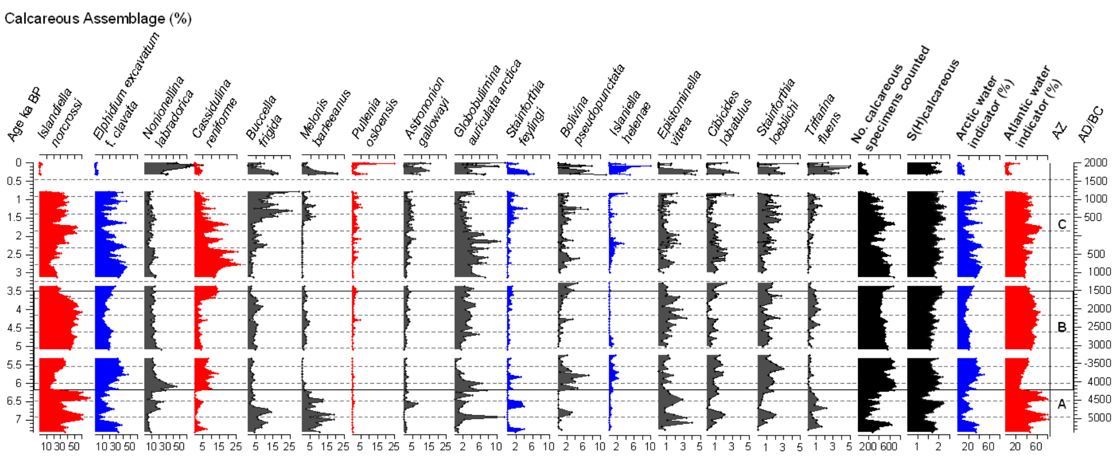

Figure 6

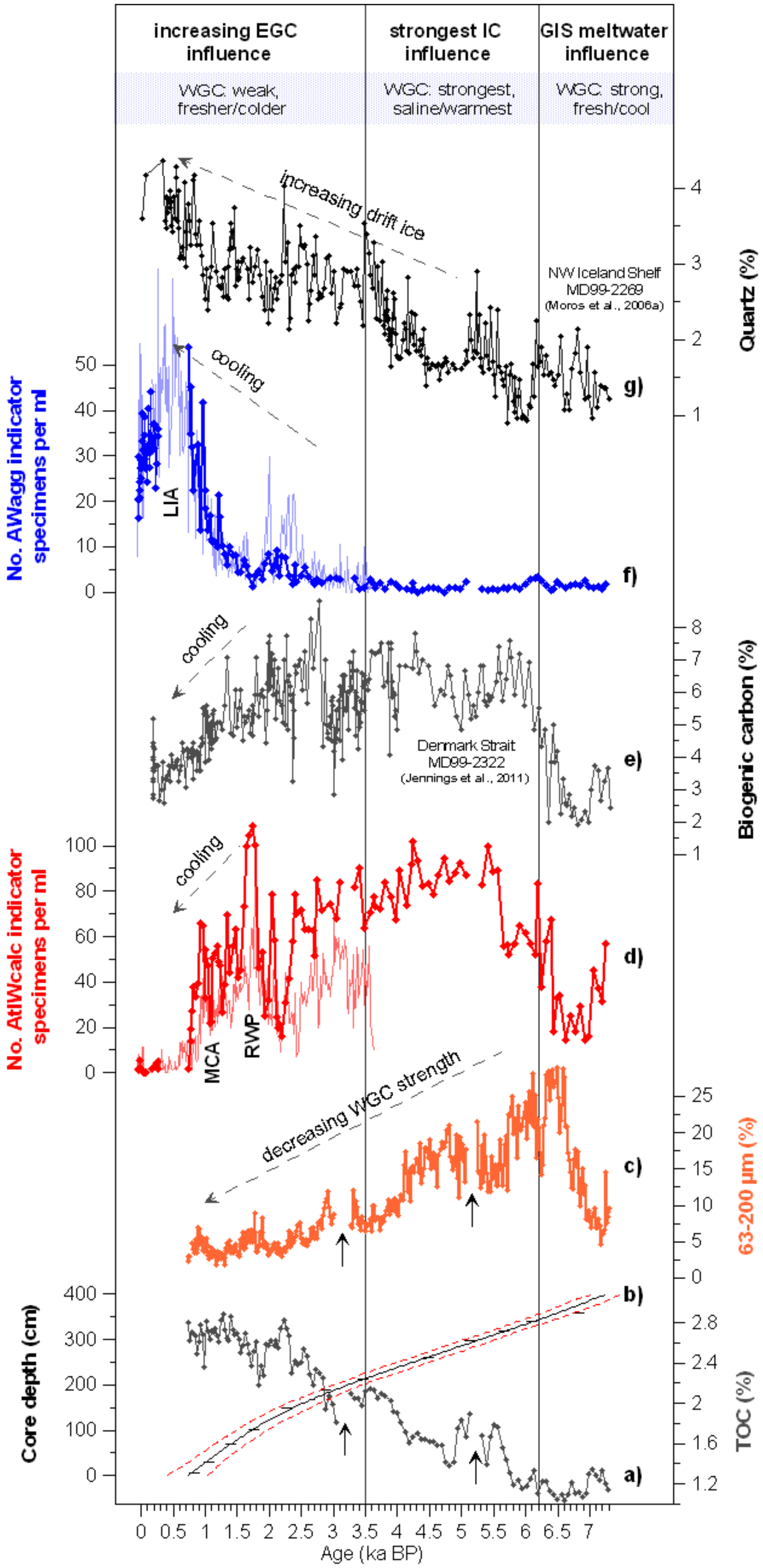

increasing EGC influence
strongest IC influence
GIS meltwater influence
WGC: weak, fresher/colder
WGC: strongest, saline/warmest
WGC: strong, fresh/cool
increasing drift ice
NW Iceland Shelf MD99-2269 (Moros et al., 2006a)
Quartz (%)
g)
cooling
No. AWagg indicator specimens per ml
LIA
f)
cooling
Denmark Strait MD99-2322 (Jennings et al., 2011)
Biogenic carbon (%)
e)
cooling
No. AtlWcalc indicator specimens per ml
MCA
RWP
d)
decreasing WGC strength
63-200 µm (%)
c)
b)
Core depth (cm)
TOC (%)
a)
Age (ka BP)

Table 1 Radiocarbon dates for gravity core 343300. Uncertainties include 68% of the probability distribution.

Depth (cm)	**Lab. Code**	**Material**	**Mass mgC**	**^{14}C date years BP**	**Calibrated yrs BP 1950 ΔR 140±35**	**Years (AD/BC)**
MUC 343300-2 (Lloyd et al., 2011)						
26.5	Poz-35009	Mix benthic foraminifera	NA	700±30	140-260	AD 1810-1690
GC 343300-3						
5.5	Poz-39052	Mix benthic foraminifera	NA	1415±35	767-885	AD 1183-1065
30	Poz-39051	Mix benthic foraminifera	NA	1645±30	990-1117	AD 960-833
71	Poz-33489	Mix benthic foraminifera	NA	1990±50	1324-1466	AD 626-484
100.5	Poz-39047	Mix benthic foraminifera	NA	2305±30	1697-1817	AD 253-133
149.5	Poz-39048	Mix benthic foraminifera	NA	2750±60	2167-2353	217-403 BC
169.5	Poz-43445	Mix benthic foraminifera	NA	3005±35	2561-2713	611-763 BC
190	AA-81304	paired *Yoldia limatula*	NA	3248±44	2800-2953	850-1003 BC
213.5	Poz-30985	*G.auriculata arctica* & *N. labradorica*	NA	3715±35	3401-3532	1451-1582 BC
219.5	Poz-43446	Mix benthic foraminifera	NA	3820±50	3507-3532	1451-1582 BC
239.5	Poz-43447	Mix benthic foraminifera	NA	4110±50	3885-4060	1935-2110 BC
261.5	Poz-33456	*G.auriculata arctica* & *N. labradorica*	NA	4490±40	4410-4555	2460-2605 BC
297.5	Poz-33457	*N. labradorica*	NA	4970±40	5041-5226	3091-3276 BC
319.5	Poz-39053	Mix benthic foraminifera	NA	5440±40	5594-5708	3644-3758 BC
340	AA-81307	*G.auriculata arctica* & *N. labradorica*	NA	5822±57	6000-6171	4050-4221 BC
359	Poz-39054	Mix benthic foraminifera	NA	6500±50	6746-6905	4796-4955 BC
399.5	Poz-39055	Mix benthic foraminifera	NA	7390±50	7649-7782	5699-5832 BC

Table 2 Benthic foraminifera included in the chilled Atlantic water species (AtlW) and Arctic water species (AW)

Atlantic Water Species (AtlW)	**References**
Agglutinated	
Adercotryma glomerata	Vilks, 1980; Jennings and Helgadóttir, 1994; Hald and Korsun, 1997; Lloyd, 2006
Ammoscalaria pseudospiralis	Vilks and Deonarine, 1988
Reophax fusiformis	Vilks, 1980; Jennings and Helgadóttir, 1994; Hald and Korsun, 1997
Reophax pilulifer	Vilks, 1980; Jennings and Helgadóttir, 1994; Hald and Korsun, 1997
Saccammina diflugiformis	Vilks, 1980; Scott and Vilks, 1991; Jennings and Helgadóttir, 1994; Hald and Korsun, 1997
Calcareous	
Cassidulina reniforme	Hald and Steinsund, 1996; Guilbault et al., 1997
Pullenia osloensis	Wollenburg et al., 2004
Islandiella norcrossi	Vilks, 1980; Mudie et al., 1984; Hald and Korsun, 1997; Duplessy et al., 2001; Lloyd, 2006
Arctic Water species (AW)	
Agglutinated	
Cuneata arctica	Madsen and Knudsen, 1994, Jennings et al., 2001; Lloyd, 2006
Spiroplectammina biformis	Schafer and Cole, 1986; Jennings and Helgadóttir, 1994; Madsen and Knudsen, 1994; Korsun and Hald, 2000
Textularia torquata	Ishman and Foley, 1996
Calcareous	
Elphidium excavatum f. *clavata*	Hald and Korsun, 1997; Osterman and Nelson, 1989; Vilks et al., 1989
Islandiella helenae	Korsun and Polyak, 1989; Steinsund et al., 1994
Stainforthia feylingi	Knudsen and Seidenkrantz, 1994

Supplementary figure captions

Figure S1: Agglutinated foraminiferal assemblage from site 343300 versus age. Foraminiferal frequencies are expressed as total number of agglutinated specimens counted per ml wet sediment. Blue (red) colored species are included in the AW (AtlW) group.

Figure S2: Calcareous foraminiferal assemblage of site 343300. Foraminiferal frequencies are expressed as total number of calcareous specimens counted per ml wet sediment. Blue (red) colored species are included in the AW (AtlW) group.

Figure S1

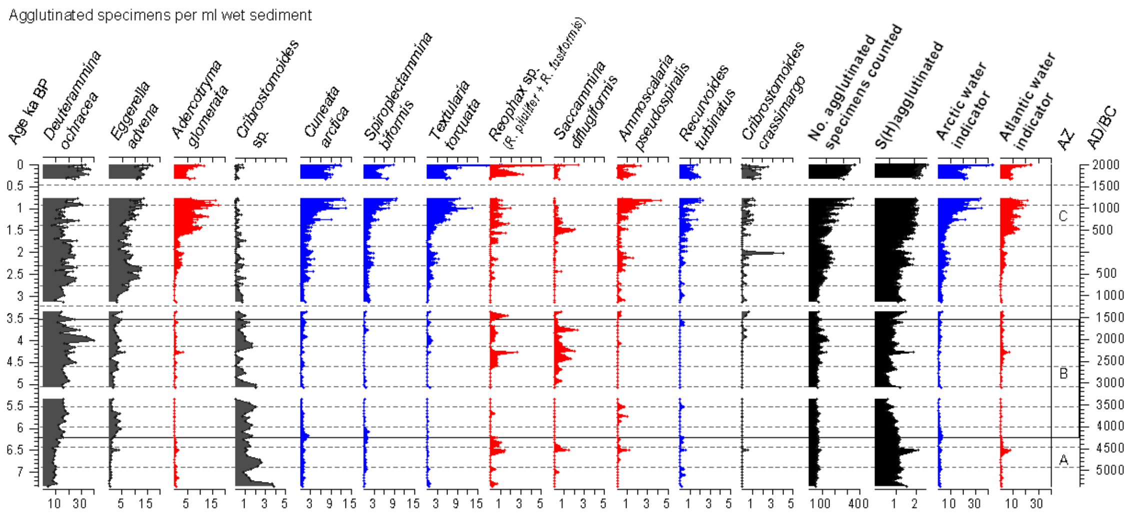

Figure S2

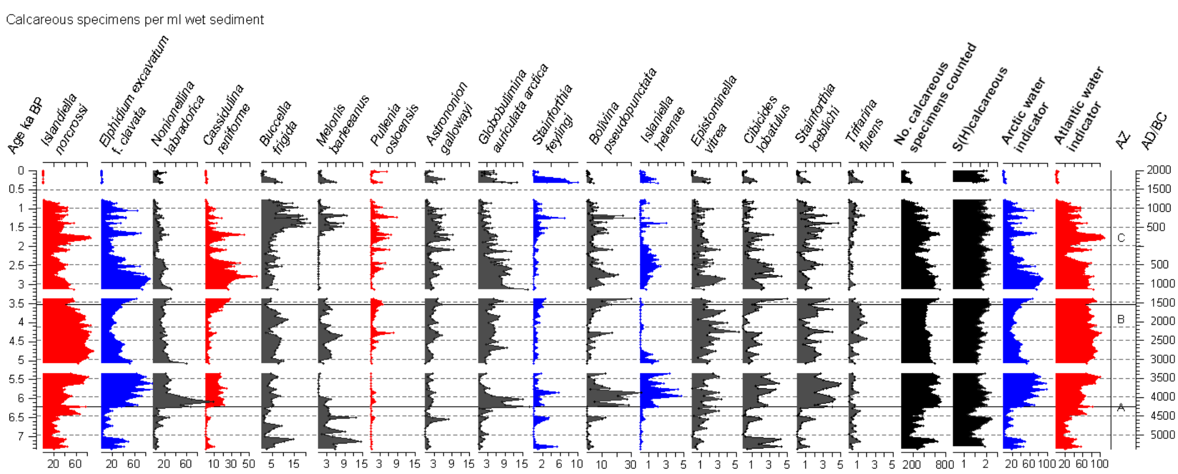

966